Compensation of low-frequency noise induced by power line in trapped-ion system

Han Hu
National University of Defense Technology
Yi Xie
National University of Defense Technology
Man-chao Zhang
National University of Defense Technology
Qing-qing Qin
National University of Defense Technology
Jie Zhang
National University of Defense Technology
Wen-bo Su
National University of Defense Technology
Tian-xiang Zhan
National University of Defense Technology
Chun-wang Wu
National University of Defense Technology
Ping-xing Chen
National University of Defense Technology
Wei Wu (weiwu@nudt.edu.cn)
National University of Defense Technology

Research Article

Keywords:

Posted Date: May 9th, 2022

DOI: https://doi.org/10.21203/rs.3.rs-1608974/v1

myjournal manuscript No.
(will be inserted by the editor)

Compensation of low-frequency noise induced by power line in trapped-ion system

Han Hu[1,⋆], Yi Xie[1,⋆], Man-chao Zhang[1], Qing-qing Qin[1], Jie Zhang[1], Wen-bo Su[1], Tian-xiang Zhan[1], Chun-wang Wu[1], Ping-xing Chen[1], Wei Wu[1] ⋆⋆

Department of Physics, College of Liberal Arts and Sciences, National University of Defense Technology, Changsha, 410073, P. R. China

Received: date / Revised version: date

Abstract The low-frequency magnetic field noise resulting from the laboratory power supply is one of the main decoherence sources of trapped-ion qubits. Synchronizing the experimental sequence to the phase of the power line is widely used to mitigate this problem, but it will greatly reduce the experimental efficiency. In this paper, we experimentally demonstrate a simple active compensation method to reduce the observed 50 Hz and 150 Hz strong magnetic noise in an ion trap induced by the power line. In our method, a single $^{40}Ca^{+}$ ion is used as the noise probe and an reverse compensation signal is generated by a programmable arbitrary waveform generator (AWG).

⋆ these authors contributed equally to this work.
⋆⋆ weiwu@nudt.edu.cn

After compensation, an 86% reduction of the periodic magnetic field fluctuation and over 35-fold extension of the coherence time from 70 µs to 2500 µs were observed. This method can also be applied to compensate other spectral components of the magnetic field noise related to the power line, and it is also useful for other atomic systems such as neutral atoms.

1 Introduction

The trapped-ion system has been proven to be a promising candidate for quantum computing [1–3]. In the implementation of trapped-ion quantum computing, qubits can be encoded in a two-level system formed by the electronic ground and the long-lived excited state of an ion. The realization of quantum computing requires that the encoded states have long enough relaxation time and coherence time to complete the required quantum gate operations [4–8]. However, experimentally, magnetic field noise greatly limits the coherence time of ion qubits, especially for those optical qubits [9, 10]. The ambient magnetic field results in a fluctuating shift of the qubit's energy levels via Zeeman effect. The noise spectrum of the ambient magnetic field is expected to have a strong correlation with the power line frequency of 50 Hz. Experimental cycles can be synchronized with the power line to reduce the influence of 50 Hz noise and prolong the coherence time of ion qubits [9], but this line trigger method limits the time of each experimental cycle to 20 ms, which reduces the experimental efficiency. In addition, line trigger does not really eliminate the magnetic field jitter, and the energy level will

still shift during one quantum operation cycle, which is even worse when the operation time is long.

Magnetic shielding is an effective method to solve this problem. However, it will occupy a large space and often reduces the optical access [11, 12]. Besides, the magnetic shielding has less suppression for the low frequency noise [13]. In addition to passive compensation methods, a common approach is using magnetometers to actively monitor the magnetic field noise and then compensate it, but its compensation effect is imperfect due to its imperfect measurement position [14–16]. Moreover, feedback and feedforward circuits are employed to suppress the magnetic field noise, but the circuit design is very complicated [17].

In this paper, a simple scheme of using a programmable signal source to compensate the low-frequency magnetic field noise in the center of the trap is proposed. For convenience, we choose an arbitrary waveform generator (AWG) as a demonstration, which can generate modulation signal composed of the 50 Hz sine wave and its harmonic components. In the experiment, a single $^{40}Ca^{+}$ ion is used as a probe to detect the magnetic field noise at trap center and the result is used to optimize the parameters of modulation signal. By measuring the variation of atomic transition frequency over one cycle of the power supply, it is observed that magnetic field noise fluctuation is reduced to 14%. By measuring the coherence time T_2^* with the standard Ramsey experiments [18], a 35-fold extension of the coherence time is observed from 70 µs to 2500 µs without using the line trigger.

2 Compensation scheme and experimental setup

Mains electricity in the laboratory is usually transmitted through a three-phase alternating current (AC) system. Different loads generate the third (and higher) harmonic current in the neutral conductor, yielding not only 50 Hz but also a strong noise component of 150 Hz [19]. In our experiment, the desired magnetic field of the trapped-ion system is produced by permanent magnets, which are not the source of magnetic field noise. So we deduce it is the magnetic field emitted by the power line that leads to the time varying Zeeman shift of the energy levels, which leads to the loss of coherence. We measured the variation of atomic transition frequency over one cycle of power line and verified that the magnetic field noise is a stable periodic signal. Note that in trapped-ion system, only the magnetic field noise at the trap center is concerned. Therefore, we can use the trapped ion as a probe and compensate the magnetic field noise at its position by an intuitive active compensation method.

As shown in Fig. 1, the main devices used in our scheme are a three-turn magnetic field compensation coil and a programmable AWG (Keysight 33600A). The compensation coil is installed in the direction of the main magnetic field. The AWG can generate multi-frequency superimposed signals with different phases, and drives the coil to produce an alternating magnetic field to compensate the noise along the magnetic field direction at the position of the ion. In the experiment, a single $^{40}Ca^{+}$ ion is used to probe the magnetic field, which is loaded into the blade-shaped linear

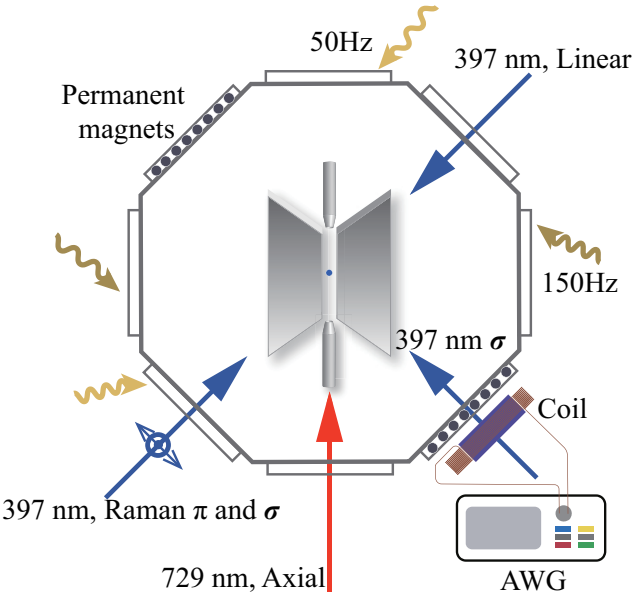

Fig. 1 Schematic view of the experimental setup. The black dots represent permanent magnets used to generate the main magnetic field. The compensation magnetic field coil is installed in the direction of the quantum polarization axis and powered by an AWG. The copropagating Raman σ and π beams are used to manipulate the qubit. The 397 nm linear beam is for the Doppler cooling and fluorescence detection. The 397 nm σ laser beam is used to initialize the ion quantum state to $S_{1/2}(m_J = -1/2)$. The 729 nm axial beam is used to shelve the $S_{1/2}(m_J = -1/2)$ state to $D_{5/2}$ state for the fluorescence detection. The wave lines are the low-frequency magnetic field noise induced by the power line.

Paul trap by applying the three-step photoionization method with 732 nm and 423 nm laser beams [20]. The qubit is usually encoded in a ground state and a metastable state of $^{40}Ca^{+}$ ions, but the laser frequency noise will also be a problem that affects the coherence time [21]. In our experiment, the spin qubit is encoded in the ground states of the Zeeman sublevels

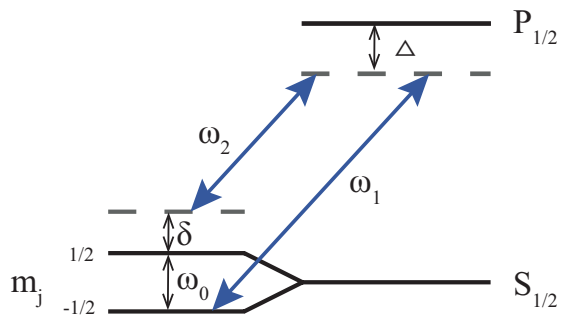

Fig. 2 Scheme of the stimulated Raman transitions for a $^{40}Ca^{+}$ ion. The Zeeman sublevels of the ground state are split by 10.057 MHz. The effective detuning δ from the transition $S_{1/2}(m_J = -1/2) \leftrightarrow S_{1/2}(m_J = 1/2)$ is given by $\omega_1 - \omega_2 = \omega_0 + \delta$. Both beams are detuned to the two-level resonance frequency by $\Delta = -180$ GHz.

$S_{1/2}(m_J = -1/2)$ and $S_{1/2}(m_J = 1/2)$, which have a frequency gap about 10 MHz and can be manipulated directly by Raman transitions [22, 23]. As shown in Fig. 2, the two-photon stimulated Raman transition is driven by two 397 nm laser beams with detuning $\Delta = -180$ GHz [24, 25]. Since both Raman beams are generated from the same laser and copropagating to the ion, the Raman transition linewidth is insensitive to the laser frequency jitter [23, 26]. Therefore, the magnetic field noise becomes the primary factor that restricts the coherence time of ion qubits. Besides, both Raman beams propagate in the same optical fiber, so the effective wave-vector of Raman beams is zero and the Raman transitions are insensitive to the ion's motion [23], therefore the motional decoherence would not involved in our experiment.

The typical experimental sequence in our scheme starts with Doppler cooling of a single $^{40}Ca^{+}$ ion. Subsequently, by applying 397 nm σ^{-} laser pulse, the ion can be initialized to $S_{1/2}(m_J = -1/2)$. Then, the spin qubit can be manipulated by two red-detuned 397 nm laser beams. To distinguish the qubit states ($S_{1/2}(m_J = -1/2)$ and $S_{1/2}(m_J = 1/2)$), electron shelving technique [27] is employed, where a frequency-selective laser pulse near 729 nm is used to transfer $S_{1/2}(m_J = -1/2)$ to the metastable $D_{5/2}$ before applying the detection beams.

In order to quantitatively measure low-frequency noise, we use line trigger to synchronize experimental sequence to the phase of the power line and obtain the Raman transition frequency shift as a function of different delay time relative to the power signal, which could be used as symbol of magnetic field noise. To check whether the magnetic field noise is suppressed by our method, the variation of resonance frequency during one cycle of the power line signal is recorded before and after compensation. Besides, the dephasing time of ion qubits affected by the magnetic field noise is also measured by scanning the free evolution time in the Ramsey experiment.

3 Results and analysis

Firstly, the background magnetic field induced resonance frequency shift with different delay time is quantitatively measured by using above setup. The result is shown in Fig. 3(a), magnetic field noise induced by the power line causes a frequency shift magnitude of about 7 kHz, indicating 2.5 mG

magnetic noise amplitude. To extract the amplitude and phase for 50 Hz and its harmonics, nonlinear fitting was carried out with frequency components including 50 Hz, 100 Hz, 150 Hz and 200 Hz. The fitting function is

$$f = A + \sum_{i=1}^{4} B_i \cos(2\pi * 50i * t + \phi_i), \tag{1}$$

where f represents carrier transition frequency. $B_i (i = 1, 2, 3, 4)$ denote the amplitude of the i-th order harmonics, t is the phase delay time of power line, and $\phi_i (i = 1, 2, 3, 4)$ are the initial phase respectively.

As shown in Table 1, we obtain the amplitudes of noise at each frequency and find that 50 Hz and 150 Hz are the main components of magnetic field noise. These strong noises greatly affect the coherence time of ion qubits. Fig. 3(b) shows the measurement results of Ramsey fringes with transition $S_{1/2}(m_J = -1/2) \leftrightarrow S_{1/2}(m_J = 1/2)$. The probability of each point is obtained by averaging 100 experiments and the fitting function [28] is

$$P_S = \frac{1}{2}[\exp(-\tau^2/T_2^{*2}) \cos(\omega\tau + \phi_j) + 1], \tag{2}$$

where P_S denotes the population of $S_{1/2}(m_J = 1/2)$ state, ω is the oscillation frequency of the fringe, τ is the free precession time, ϕ_j is the phase offset and T_2^* is the coherence time. Without line trigger and reverse compensation, the coherence time T_2^* extracted is around 70 μs.

To suppress the major components of the magnetic field noise, we implement reverse compensation for 50 Hz and 150 Hz noises in this paper. An out-of-phase compensation signal is generated by applying proper driving signal to the compensation magnetic coil via an AWG. The driving signal is

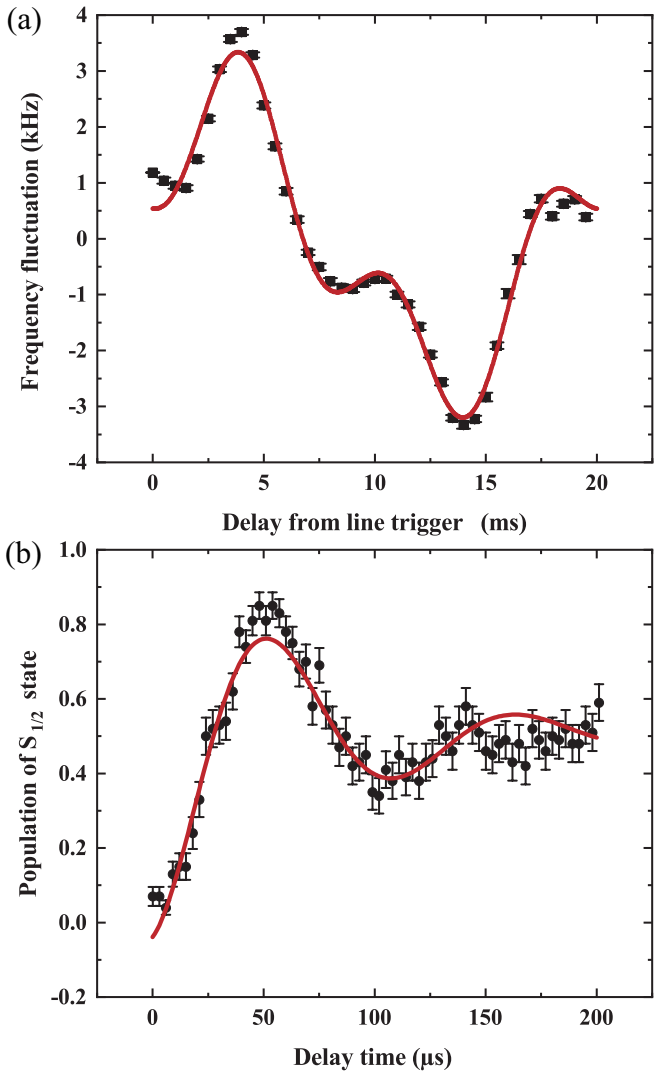

Fig. 3 (a) The central frequency fluctuation with the phase of 50 Hz signal. The red line indicates the fitted curve with empirical formula Eq. (1) and the error bars show the error of its center frequency. The power line introduces a resonance frequency fluctuation of about 7 kHz on this spectral line. (b) Ramsey interference fringes of transition $S_{1/2}(m_J = -1/2) \leftrightarrow S_{1/2}(m_J = 1/2)$. The solid line is the fitting using empirical function Eq. (2), where the probability of each point is obtained by averaging 100 experiments. Without line trigger, the coherence time T_2^* is around 70 μs. The error is calculated by projection measurement noise model.

Table 1 The amplitude of changes in resonance frequency induced by noise components at 50 Hz, 100 Hz, 150 Hz and 200 Hz.

Frequency (Hz)	50	100	150	200
Amplitude (kHz)	2.329	0.067	1.046	0.038

derived through an excitation-response process. We give the compensation coil a sinusoidal excitation signal slightly shorter than 20 ms, with frequency of 50 Hz and 150 Hz, phase zero and predefined amplitude, which is triggered by the power line synchronization signal, and obtain the fluctuation of Raman transition frequency over the phase delay time of power line. So the response of the compensation coil to the excitation signal can be obtained by subtracting the frequency fluctuation caused by background magnetic field noise. The changed resonance frequency caused by the excitation signal is regarded as the response of excitation. According to the relationship between background noise and excitation signal, the amplitude and phase of the compensating driving signal can be derived. In the experiment, we found that the magnetic field coil responds to input signal in a non-linear

manner, and the driving signal could be modified more accurately. For this purpose, we iteratively modify the driving signal, in each iteration, the dephasing time is measured and used to judge the modification. The process is terminated until the coherence time is optimal. As shown in Fig. 4(b), it can be found that the longest coherence time can reach about 2500 µs which is 35.7 times longer than that before applying the reverse modulation signal. It can be seen that the experimental data points are in good agreement with the fitting curve, and the spectrum of dephasing noise obeys Gaussian distribution.

The fluctuation of carrier resonant frequency with the phase delay to power line is shown in Fig. 4(a). It can be seen that the fluctuation of frequency tends to be smooth and obviously improved by our method.

4 Discussion and conclusion

In this work, a programmable AWG was used to generate multi-frequency sinusoid wave compensation signal containing 50 Hz and 150 Hz components to suppress magnetic field noise, which increases the coherence time of a $^{40}Ca^{+}$ single qubit from 70 µs to 2500 µs. By measuring the fluctuation of Raman transition frequency over the phase delay time of power line before and after suppression, the fluctuation amplitude of carrier frequency, i.e. the amplitude of magnetic field noise is reduced by about one order compared with the case without suppression. Of course, after determining the parameters, we can use a programmable signal source with low

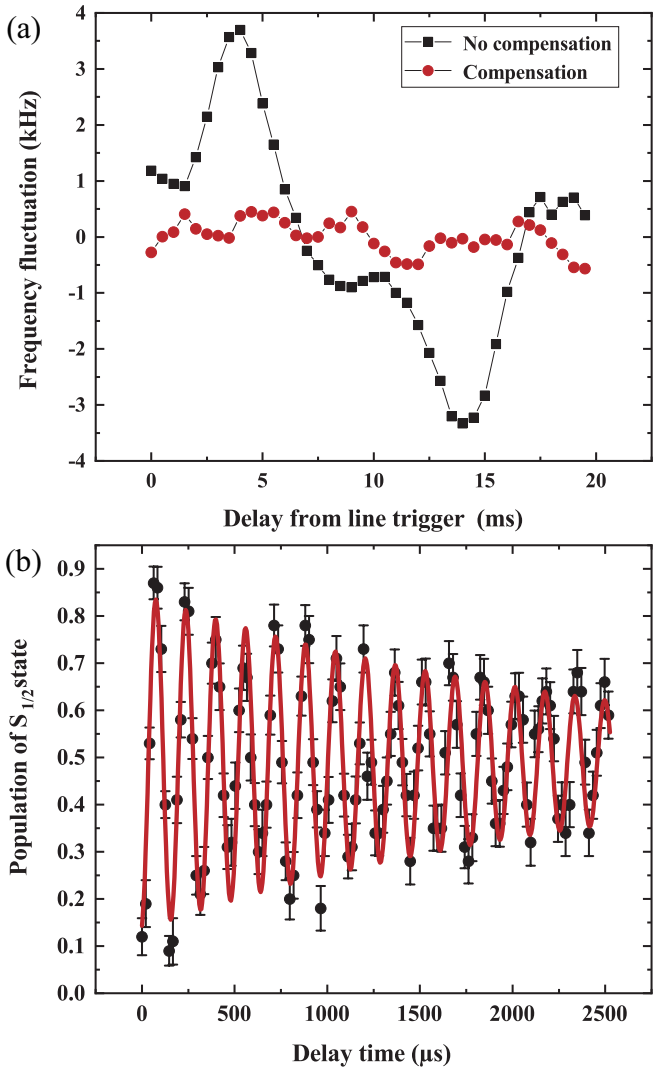

Fig. 4 (a) Experimental results of the fluctuation of carrier resonance frequency with the phase delay of power line before and after compensation. The black squares show the relationship between the central frequency fluctuation of Raman transition and the phase of 50 Hz mains. The red dots indicate the frequency drift after the stray magnetic field is cancelled. After compensation, the ion magnetic field noise is suppressed by about 86%. (b) Ramsey interference fringes for transition $S_{1/2}(m_J = -1/2) \leftrightarrow S_{1/2}(m_J = 1/2)$, without line trigger. The solid line is the fitting curve using function Eq. (2) and the coherence time T_2^* extracted is around 2.5 ms. The error is calculated by projection measurement noise model.

sampling rate to replace the AWG. Besides, our compensation scheme does not require complex feedback circuits or additional magnetic field detection devices. But in the experiment, if we keep the line trigger on, the coherence time can reach 8 ms. It means that the work reported here is far from eliminate the periodic magnetic field noise, which may due to the deficiencies in our implementation: (i) We only compensated the stray magnetic fields components of 50 Hz and 150 Hz, while similarly, the other order harmonics can also be compensated if necessary. (ii) The response of the coil to the input signal is nonlinear, which makes the perfect compensation complicated. (iii) The data fitting is not very accurate, when we measure the variation of magnetic field noise with time. So the line trigger can be removed only the quantum state operation time is short in this paper.

Acknowledgements This work is supported by the National Natural Science Foundation of China (Grant Nos. 11904402, 12074433, 12004430, 12174447, and 12174448).

References

1. J.I. Cirac, P. Zoller, Phys. Rev. Lett. **74**, 4091 (1995)
2. G. Pagano, P.W. Hess, H.B. Kaplan, W.L. Tan, P. Richerme, P. Becker, A. Kyprianidis, J. Zhang, E. Birckelbaw, M.R. Hernandez, Y. Wu, C. Monroe, Quantum Science and Technology **4**, 014004 (2018)
3. C. Monroe, J. Kim, Science **339**, 1164 (2013)
4. F. Schmidt-kaler, H. Häffner, M. Riebe, S. Gulde, G.P.T. Lancaster, T. Deuschle, C. Becher, C.F. Roos, J. Eschner, R. Blatt, Nature **422**,

408 (2003)

5. M. Riebe, H. Häffner, C.F. Roos, W. Hänsel, J. Benhelm, G.P.T. Lancaster, T.W. Körber, C. Becher, F. Schmidt-Kaler, D.F.V. James, Nature **429**, 734 (2004)
6. T. Monz, K. Kim, W. Hänsel, M. Riebe, A.S. Villar, P. Schindler, M. Chwalla, M. Hennrich, R. Blatt, Phys. Rev. Lett. **102**, 040501 (2009)
7. T. Monz, P. Schindler, J.T. Barreiro, M. Chwalla, D. Nigg, W.A. Coish, M. Harlander, W. Hänsel, M. Hennrich, R. Blatt, Phys. Rev. Lett. **106**, 130506 (2011)
8. H. Häffner, W. Hänsel, M. Riebe, C.F. Roos, J. Benhelm, D. Chek-al kar, M. Chwalla, T. Körber, U.D.M. Rapol, P.O. Schmidt, C. Becher, O. Gühne, W. Dür, R. Blatt, Nature **438**, 643 (2005)
9. F. Schmidt-Kaler, S. Gulde, M. Riebe, T. Deuschle, A. Kreuter, G. Lancaster, C. Becher, J. Eschner, H. Häffner, R. Blatt, Journal of Physics B: Atomic, Molecular and Optical Physics **36**, 623 (2003)
10. C.F. Roos, M. Chwalla, K. Kim, M. Riebe, R. Blatt, Nature **443**, 316 (2006)
11. T. Ruster, C.T. Schmiegelow, H. Kaufmann, C. Warschburger, F. Schmidt-Kaler, U.G. Poschinger, Appl. Phys. B **122**, 254 (2016)
12. M. Brandl, M. Van Mourik, L. Postler, A. Nolf, K. Lakhmanskiy, R. Paiva, S. Möller, N. Daniilidis, H. Häffner, V. Kaushal, et al., Review of Scientific Instruments **87**, 113103 (2016)

13. R. Zhang, Y. Ding, Y. Yang, Z. Zheng, J. Chen, X. Peng, T. Wu, H. Guo, Sensors **20**, 4241 (2020)
14. C.J. Dedman, R. Dall, L. Byron, A. Truscott, Review of scientific instruments **78**, 024703 (2007)
15. A. Laraoui, J.S. Hodges, C.A. Meriles, Applied Physics Letters **97**, 143104 (2010)
16. W. Wei, P. Hao, Z. Ma, H. Zhang, L. Pang, F. Wu, K. Deng, J. Zhang, Z. Lu, Journal of Physics B: Atomic, Molecular and Optical Physics **55**, 075001 (2022)
17. B. Merkel, K. Thirumalai, J. Tarlton, V. Schäfer, C. Ballance, T. Harty, D. Lucas, Review of Scientific Instruments **90**, 044702 (2019)
18. N.F. Ramsey, Phys. Rev. **76**, 996 (1949)
19. C. Hempel, Digital quantum simulation, schrödinger cat state spectroscopy and setting up a linear ion trap. Ph.D. thesis (2014)
20. J. Zhang, Y. Xie, P.f. Liu, B.q. Ou, W. Wu, P.x. Chen, Appl. Phys. B **123**, 45 (2017)
21. M. Zhang, Y. Xie, J. Zhang, W. Wang, C. Wu, T. Chen, W. Wu, P. Chen, Phys. Rev. Applied **15**, 014033 (2021)
22. F. Mintert, C. Wunderlich, Phys. Rev. Lett. **87**, 257904 (2001)
23. C. Monroe, D.M. Meekhof, B.E. King, W.M. Itano, D.J. Wineland, Phys. Rev. Lett. **75**, 4714 (1995)
24. C. Monroe, D.M. Meekhof, B.E. King, S.R. Jefferts, W.M. Itano, D.J. Wineland, P. Gould, Phys. Rev. Lett. **75**, 4011 (1995)

25. D.J. Wineland, C. Monroe, W.M. Itano, D. Leibfried, B.E. King, D.M. Meekhof, Journal of Research of the National Institute of Standards and Technology **103**, 259 (1998)
26. J.E. Thomas, P.R. Hemmer, S. Ezekiel, C.C. Leiby, R.H. Picard, C.R. Willis, Phys. Rev. Lett. **48**, 867 (1982)
27. C. Roos, T. Zeiger, H. Rohde, H.C. Nägerl, J. Eschner, D. Leibfried, F. Schmidt-Kaler, R. Blatt, Phys. Rev. Lett. **83**, 4713 (1999)
28. J. Zhang, W. Wu, C.w. Wu, J.g. Miao, Y. Xie, B.q. Ou, P.x. Chen, Appl. Phys. B **126**, 20 (2020)